

Fine Structure in Proton Emission from ^{145}Tm Discovered with Digital Signal Processing

M. Karny,^{1,2} R. K. Grzywacz,^{1,3} J. C. Batchelder,⁴ C. R. Bingham,^{2,3} C. J. Gross,^{3,5} K. Hagino,⁶ J. H. Hamilton,⁷ Z. Janas,^{1,8} W. D. Kulp,⁹ J. W. McConnell,^{3,8} M. Momayezi,¹⁰ A. Piechaczek,¹¹ K. P. Rykaczewski,^{1,3} P. A. Semmes,¹² M. N. Tantawy,² J. A. Winger,¹³ C. H. Yu,³ and E. F. Zganjar¹¹

¹*IFD, Warsaw University, Pl-00681 Warsaw, Hoża 69, Poland*

²*University of Tennessee, Knoxville, Tennessee 37996*

³*Physics Division, ORNL, Oak Ridge, Tennessee 37830*

⁴*UNIRIB, Oak Ridge Associated Universities, Oak Ridge, Tennessee 37831*

⁵*Oak Ridge Institute for Science and Education, Oak Ridge, Tennessee 37831*

⁶*Yukawa Institute for Theoretical Physics, Kyoto University, Kyoto 606-8502, Japan*

⁷*Department of Physics, Vanderbilt University, Nashville, Tennessee 37235*

⁸*Joint Institute for Heavy Ion Research, Oak Ridge, Tennessee 37831*

⁹*Department of Physics, Georgia Institute of Technology, Atlanta, Georgia 30332*

¹⁰*X-Ray Instrumentation Associates, Newark, California 94560*

¹¹*Department of Physics, Louisiana State University, Baton Rouge, Louisiana 70803*

¹²*Department of Physics, Tennessee Technological University, Cookeville, Tennessee 38505*

¹³*Department of Physics, Mississippi State University, Mississippi State, Mississippi 39762*

(Received 29 July 2002; published 7 January 2003)

Fine structure in proton emission from the $3.1(3) \mu\text{s}$ activity of ^{145}Tm was discovered by using a novel technique of digital processing of overlapping recoil implantation and decay signals. Proton transitions to the ground state of ^{144}Er and to its first excited 2^+ state at $0.33(1) \text{ MeV}$ with a branching ratio $I_p(2^+) = 9.6 \pm 1.5\%$ were observed. The structure of the ^{145}Tm wave function and the emission process were analyzed by using particle-core vibration coupling models.

DOI: 10.1103/PhysRevLett.90.012502

PACS numbers: 23.50.+z, 21.10.Pc, 21.10.Tg, 27.60.+j

Studies of proton radioactivity, which started over 30 years ago with the discovery of the proton-emitting isomer ^{53m}Co [1], are providing unique information on the structure of nuclei beyond the stability limits [2–4]. The proton emission rate is strongly dependent on the decay energy and on the angular momentum of the emitted proton. Utilizing the precisely measured decay energies and partial proton emission half-lives, one can understand the relative energies, spins, and parities of single-particle proton orbitals beyond the proton drip line, especially for spherical nuclei [5]. However, the deformation of the nuclear potential plays an important role in the proton emission process. The complex structure of the wave function can reduce the decay probabilities expected within the simple spherical picture as shown by studies on proton radioactivities in the deformed rare-earth region [6,7]. The observation of fine structure in proton emission is particularly interesting since it reveals additional properties of the wave function of the proton-unbound state. In the case of an (odd- Z , even- N) emitter the proton transition to the 0^+ ground state dominates and observation of a weak transition to the $I^\pi = 2^+$ first excited state of the even-even daughter nucleus is challenging. The measured energy of this 2^+ level allows us to estimate the quadrupole deformation [8,9] of the potential tunneled by the protons and the relative intensity gives information on the composition of the wave function.

Prior to this work only one such observation of proton fine structure was published [10], the decay of highly deformed ^{131}Eu ($\beta_2 \approx 0.3$). Our Letter presents the first evidence for fine structure in proton emission from a transitional nucleus ^{145}Tm ($\beta_2 \approx 0.18$) and its analysis within the particle-core vibration coupling models. This very exotic nucleus, located four mass units beyond the proton drip line, has the shortest half-life ($\approx 3 \mu\text{s}$ [11]) measured to date for proton radioactivity. The identification of $^{145}\text{Tm}^{+27}$ [11] was based on about 50 proton events at an energy of $1.728(10) \text{ MeV}$, recorded at the rate of about one event per hour.

During the first study and present experiment the ^{145}Tm ions were produced in a $^{58}\text{Ni}(315 \text{ MeV}, 15 \text{ pA}) + ^{92}\text{Mo}(0.9 \text{ mg/cm}^2)$ reaction with a cross section $\sigma \approx 0.5 \mu\text{b}$. Recoiling ions having a kinetic energy around 103 MeV were separated by the Recoil Mass Separator (RMS) [12] at Oak Ridge during a $2.2 \mu\text{s}$ flight to the final focus, where they were implanted in a double-sided silicon strip detector (DSSD), after triggering a position sensitive avalanche gas counter (PSAC) and being slowed down by a degrader foil.

The development of a novel signal processing technique was critical for a search for a weak proton branch to the excited 2^+ state. With the analog electronics [11,13,14] used in the first study of ^{145}Tm most of the fast decay events were not registered because of the amplifier overload from the 35 MeV implantation signals.

The detection of decay was blocked for about 10 μs after the implantation of $A = 145$ ions. To increase our counting efficiency for short-lived radioactivities, improvements were made to the RMS ion optics and to the detection system. In the present experiment the recoiling ions with two neighboring charge states, $Q = +26$ and $Q = +27$, were focused at the DSSD (converging solution for the ion optics [12]), increasing the overall recoil transmission ϵ_{RMS} to about 5%, i.e., by a factor of ≈ 1.5 . The main efficiency gain (a factor ≈ 7) came from a new method of detector signal processing [15–17]. The new data acquisition system is based on the four-channel digital gamma finder (DGF) modules [16]. Each DGF channel digitizes independently the amplitude of incoming preamplifier signals, in 25-ns steps. This method removes the amplifier stage of the analog electronics, thereby eliminating the overload problem. As can be seen in Fig. 1, our detection threshold is now below 1 μs of recoil-decay correlation time.

A dedicated triggering mode, designed for the study of very short-lived particle emitters and nicknamed “proton catcher,” was implemented to the DGF boards. Information was recorded as a 25- μs long digital image of the signal. The DGF recognized pileup signals in the DSSD, e.g., a 1.73 MeV proton signal on top of the ^{145}Tm ion implantation signal, within 10 μs from each other.

Events not piled up within 10 μs , however, are rejected within this DGF data acquisition mode. The fact that *only* pileup wave forms were stored dramatically reduced the data stream and dead time of the acquisition, resulting in about one readout per second at a few kHz rate of implanted ions.

Each strip of the DSSD detector was calibrated by using an external ^{241}Am alpha source, and automatic baseline and gain matching procedures were used. This calibration was tested and fine-tuned off-line with the

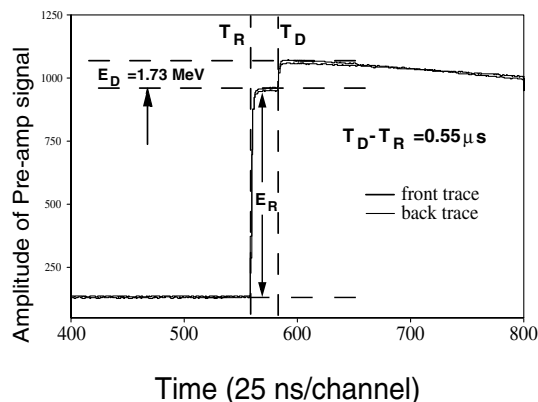


FIG. 1. Part of the preamplifier signal traces recorded by the front and the back strip of the 65- μm DSSD during the ^{145}Tm experiment. The recoil depositing about 14 MeV energy is followed after 0.55 μs by the 1.73 MeV signal. Note the perfect match, in real time, of front and back strip traces.

proton transition at 1.73 MeV [11]. One DGF module analyzed the signals from the PSAC [12] recorded with the slits set to select the ions at $A = 145$ and $Q = +26$ and $+27$. A copper degrader slowed the recoils to about 16 MeV.

The off-line data analysis started with filtering out all the traces that were qualified as valid events by the proton catcher but were actually uncorrelated or defective events, such as pileup of two implants, or a true recoil hit signal followed by an electronic noise recognized as a second event. To determine energy and time of the ion implantation and proton emission from the recorded traces, see Fig. 1, the following algorithm has been applied: (i) The implantation time T_R (left vertical dashed line) is determined by the first data point which rises above the energy threshold, in this case set to about 500 keV. (ii) The initial energy baseline is determined by the 36 data points (900 ns) prior to T_R . (iii) The total energy of the implanted ion E_R is the difference between the baseline and the maximum value within the 0.4 μs allowed for the rise time of the signal. (iv) The decay time T_D is determined by the next signal rise above the threshold value after the 0.4 μs allotted for the implantation signal (right vertical dashed line). (v) The decay energy E_D is the difference of the average of the three data points prior to T_D (decay signal baseline) and the three data points around the maximum height signal within the 0.4 μs rise time after T_D .

Once the time and energy of both pulses were calculated, the data from the front and back strips of the DSSD were compared. Events were rejected if signals coming from front and back strips did not match in time within ± 500 ns and in energy within $\pm 10\%$ of their energy average. Pileups of recoil-decay events recorded by the DSSD were validated by the presence of PSAC recoil signals matching the DSSD ion implantation time. Also, the energy of the first pulse was required to be greater than 5 MeV to be a valid recoil.

Use of these new experimental procedures gave an increase of proton counting rate from one 1.73 MeV event per hour [11] to about ten events per hour. Recorded proton signals start about 0.5 μs after the ^{145}Tm recoil implantation signal; see Figs. 1 and 2.

The total energy spectrum (summed over 32 DSSD front strips) recorded between 0.5 and 10 μs after ion implantation, shown in Fig. 3, is practically background-free. Two peaks are clearly visible above the level of proton-escape events, a dominant one at 1.728(10) MeV [11] and weaker one 0.33(1) MeV below that energy. The total number of events in the peaks recorded in the experiment are 375(19) and 40(6) counts for the 1.73 MeV and 1.40 MeV lines, respectively.

Since contributions from longer-lived β -delayed p emitters can be neglected, simple exponential decay curves were fitted to the time spectra of the 1.73 and 1.40 MeV lines (shown as insets to Fig. 3). Results of the

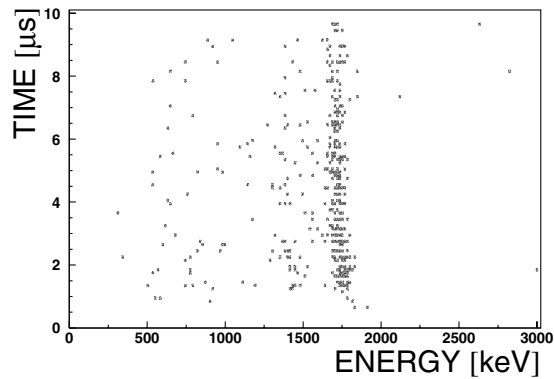


FIG. 2. The result of the valid traces analysis plotted as the energy of decay events (amplitude of the second pulse on pileup wave form) versus the recoil-decay correlation time (the time distance between the pileup pulses within the wave form). The signals recorded by the front strips are displayed, after checking the energy match within the DSSD pixel.

fits yield $T_{1/2} = 3.1 \pm 0.3 \mu\text{s}$ and $T_{1/2} = 2.7 \pm 1.0 \mu\text{s}$, respectively. Both half-lives are in agreement with the previously reported value of $3.5 \pm 1.0 \mu\text{s}$ [11], and decay events are correlated with the implantation of the $A = 145$ recoils. Therefore, we interpret them as originating from the same short-lived ^{145}Tm activity.

Since the daughter activity is an even-even nucleus, ^{144}Er , the interpretation of the 1.73 and 1.40 MeV lines as transitions to the $I^\pi = 0^+$ ground state and to the previously unknown $I^\pi = 2^+$ excited state at 0.33(1) MeV is obvious. The energy for the $I^\pi = 2^+$ state in ^{144}Er (0.33 MeV) follows the experimental systematics of the respective 2^+ energies for less exotic even-mass $N = 76$ isotones (0.347 MeV, 0.329 MeV, and 0.316 MeV for ^{138}Sm , ^{140}Gd , and ^{142}Dy , respectively). Following the valence correlation scheme $N_p N_n$ [18] one would expect ^{144}Er to have a 2^+ energy similar to that of its “ $N = 82$ mirror” nucleus ^{156}Er , which has $E(2^+) = 0.343$ MeV.

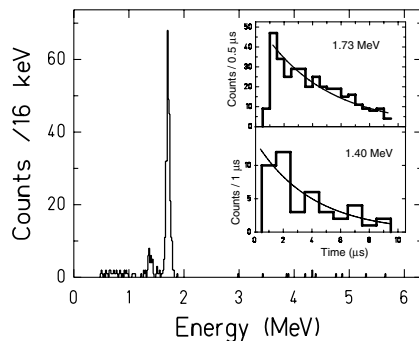


FIG. 3. Energy spectrum of decay signals derived from the analysis of recorded pileup traces. The insets show similar time dependence of the two lines observed at the energy spectrum, at 1.73 and at 1.40 MeV.

The 1.40 MeV proton pulse could sum in the DSSD with a conversion electron deexciting the 2^+ level. This effect is substantial for the ^{131}Eu decay [10], but weak for the ^{145}Tm decay. The conversion coefficient $\alpha_{\text{tot}}(E2, 0.33 \text{ MeV})$ is 5.2%. The energy resolution of the 1.73 MeV peak derived from the pileup wave form analysis is about 75 keV. Only about one to two counts in the 375-count peak may result from summing of 1.40 MeV protons with the conversion electrons from the 0.33 MeV $E2$ transition. The fine structure branching ratio is therefore obtained as $I_p(2^+) = 9.6 \pm 1.5\%$. We adopt the half-life $T_{1/2} = 3.1(3) \mu\text{s}$ following the decay pattern of the 1.73 MeV proton line measured in the present study.

Within the spherical picture allowing for the mixing of the single-particle states with particle-core vibration configurations [14,19–21], one can express the wave function of ^{145}Tm as composed mainly of $\pi 0h_{11/2}$ and $\pi 1f_{7/2}$ orbitals coupled to the 0^+ ground state and to the 2^+ excited state of the ^{144}Er core. Within a spherical approach [5], the half-lives of 1.73 MeV, $l = 5$ and 1.40 MeV, $l = 3$ proton transitions are 1.48 and 1.16 μs . Correcting for respective pairing vacancy factors u^2 of 0.647 and 0.985 [5,22] gives the $T_{1/2}$ values of 2.29 μs and of 1.18 μs , respectively, for the proton emission from $\pi 0h_{11/2}$ and $\pi 1f_{7/2}$ orbitals. These numbers can be used to derive the proton-emitting components of the ^{145}Tm wave function. To reproduce the experimental partial proton half-lives, of 3.4 μs (1.73 MeV) and of 32 μs (1.40 MeV), the presence of about 67% of $\pi 0h_{11/2} \otimes 0^+$ and about 3.7% of $\pi 1f_{7/2} \otimes 2^+$ is needed. The remaining 30% is most likely $\pi 0h_{11/2} \otimes 2^+$, and other negative parity proton orbitals coupled to the 2^+ state of the core.

However, the 2^+ energy of 0.33 MeV suggests a non-spherical shape for ^{144}Er . Both level energy evaluations, of Grodzins [8] and of Raman *et al.* [9], point to a value of $\beta_2 = 0.18$ for the quadrupole deformation parameter for ^{144}Er . Although it is not clear whether ^{144}Er is a spherical or a deformed nucleus, we may regard this β_2 as a dynamical deformation parameter around a spherical shape. Very recently, two descriptions based on particle-core vibration coupling accounting for nonspherical shapes were developed [20,21]. Following the model of Hagino [20], the composition of the wave function and respective partial decay widths calculated assuming a β_2 value of 0.18 are given in Fig. 4. The calculated half-life of $3.0(4) \mu\text{s}$ and the fine structure branching ratio of $5.7 \pm 0.3\%$ are very close to the experimental values. The fraction of the $\pi 0h_{11/2} \otimes 0^+$ component in the wave function is around 56%, similar to the spherical estimate. Fine structure in proton emission from ^{145}Tm is due to the $\approx 3\%$ presence of the $\pi 1f_{7/2} \otimes 2^+$ component. Other calculated wave function components, displayed in Fig. 4, do not contribute in a substantial way to the proton emission probability.

Calculations of Davids *et al.* [21] can reproduce the fine structure branching ratio. The value of $I_p(2^+) = 10\%$ is

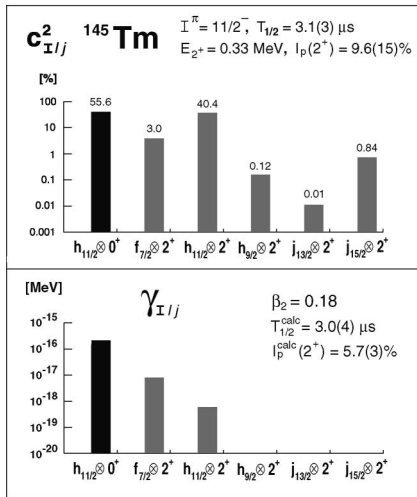


FIG. 4. The wave function structure for ^{145}Tm calculated assuming the quadrupole deformation $\beta_2 = 0.18$ within the particle-core vibration model [20] (upper panel). The coupling of single-particle proton orbitals lj to the $I = 0^+$ and $I = 2^+$ core vibration is included. The respective partial decay widths $\gamma_{I l j}$ are given in MeV (lower panel). It is clear that proton emission from ^{145}Tm is dominated by the $c^2_{0,5,11/2} = 56\%$ component of the $\pi 0 h_{11/2} \otimes 0^+$ configuration.

obtained for the model parameter $\alpha_2^{(0)}$ of 0.084. The total probability of the proton emission is close to the experimental width $\gamma = 1.5 \times 10^{-16}$ MeV. A fraction $C^2_{2,3,7/2} = 4\%$ obtained for the $\pi 1 f_{7/2} \otimes 2^+$ component is similar to the spherical estimate and the above nonspherical model results. Surprisingly the reported $C^2_{0,5,11/2} = 33\%$ [21] for the $\pi 0 h_{11/2} \otimes 0^+$ component is much lower than the spherical estimate and the particle-core vibration calculations by Hagino [20].

In summary, fine structure in proton emission with the branching ratio $I_p = 9.6 \pm 1.5\%$ was discovered during the reinvestigation of the $3.1 \mu\text{s}$ activity of ^{145}Tm . This observation was made possible by the development of the new technology of digital processing of detector signals. The slightly deformed shape, $\beta_2 = 0.18$, of the ^{144}Er potential tunneled by the emitted protons was inferred from the measured energy of 0.33 MeV for the 2^+ state. The structure of the wave function of ^{145}Tm and proton emission rates were analyzed within the models accounting for particle-core vibration coupling. The wave function was found to be dominated by the $\pi 0 h_{11/2}$ orbital coupled to the 0^+ ground state of the ^{144}Er core (about 56%) and the 2^+ excited state of the core (about 40%). The origin of the 1.40 MeV proton transition to the 2^+ state was found in the small 3% $\pi 1 f_{7/2} \otimes 2^+$ component in the wave function.

The development of a data acquisition system based on digital signal processing opens up the path to direct measurements of decay properties of very short-lived yet unknown radioactivities such as, e.g., the proton emitters ^{144}Tm , ^{149}Lu , and ^{159}Re . Because of the expanded half-life sensitivity, this detection scheme is appropriate for a search for new (super)heavy alpha emitters and two-proton radioactivities such as ^{48}Ni and ^{54}Zn . It should also allow us to measure the decay properties of ^{103}Sb , and ^{105}Te located at the island of proton and α emitters above ^{100}Sn predicted [23] as a termination region for the rp process.

ORNL is managed by UT-Battelle, LLC, for the U.S. Department of Energy under Contract No. DE-AC05-00OR22725. This work was also supported by the U.S. DOE through Contracts No. DE-FG02-96ER40983, No. DE-FG02-96ER41006, No. DE-FG05-88ER40407, No. DE-FG02-96ER40978, and No. DE-AC05-76OR00033 and by the Polish Committee for Scientific Research.

- [1] K. P. Jackson *et al.*, Phys. Lett. **33B**, 281 (1970).
- [2] S. Hofmann, Radiochim. Acta **70/71**, 93 (1995).
- [3] P. J. Woods and C. N. Davids, Annu. Rev. Nucl. Part. Sci. **47**, 541 (1997).
- [4] K. P. Rykaczewski, Eur. Phys. J. A **15**, 81 (2002).
- [5] S. Åberg *et al.*, Phys. Rev. C **56**, 1762 (1997); **58**, 3011 (1998).
- [6] C. N. Davids *et al.*, Phys. Rev. Lett. **80**, 1849 (1998).
- [7] K. Rykaczewski *et al.*, Phys. Rev. C **60**, R011301 (1999).
- [8] L. Grodzins, Phys. Lett. **2**, 88 (1962).
- [9] S. Raman *et al.*, At. Data Nucl. Data Tables **78**, 1 (2001).
- [10] A. A. Sonzogni *et al.*, Phys. Rev. Lett. **83**, 1116 (1999).
- [11] J. C. Batchelder *et al.*, Phys. Rev. C **57**, R1042 (1998).
- [12] C. J. Gross *et al.*, Nucl. Instrum. Methods Phys. Res., Sect. A **450**, 12 (2000).
- [13] P. J. Sellin *et al.*, Nucl. Instrum. Methods Phys. Res., Sect. A **311**, 217 (1992).
- [14] C. R. Bingham *et al.*, Phys. Rev. C **59**, R2984 (1999).
- [15] A. Georgiev *et al.*, IEEE Trans. Nucl. Sci. **41**, 1116 (1994).
- [16] B. Hubbard-Nelson *et al.*, Nucl. Instrum. Methods Phys. Res., Sect. A **422**, 411 (1999); <http://www.xia.com>.
- [17] R. K. Grzywacz, Nucl. Instrum. Methods Phys. Res., Sect. A (to be published).
- [18] R. F. Casten, *Nuclear Structure from a Simple Perspective* (Oxford, New York, 2000), 2nd ed., pp. 297–330.
- [19] P. B. Semmes, Nucl. Phys. **A682**, 239c (2001).
- [20] K. Hagino, Phys. Rev. C **64**, 041304R (2001).
- [21] C. N. Davids *et al.* Phys. Rev. C **64**, 034317 (2001).
- [22] W. Nazarewicz *et al.*, Nucl. Phys. **A512**, 61 (1990).
- [23] H. Schatz *et al.*, Phys. Rev. Lett. **86**, 3471 (2001).